Bull. Mater. Sci., Vol. 31, No. 3, June 2008, pp. 319–325. © Indian Academy of Sciences.

Synthesis, characterization and application of semiconducting oxide (Cu_2O and ZnO) nanostructures

D P SINGH, JAI SINGH, P R MISHRA, R S TIWARI and O N SRIVASTAVA*
Department of Physics, Banaras Hindu University, Varanasi 221 005, India

Abstract. **In the present study, we report the synthesis, characterization and application of nanostructured oxide materials. The oxide materials (Cu_2O and ZnO) have been synthesized by electrolysis based oxidation and thermal oxidation methods. Cuprous oxide (Cu_2O) nanostructures have been synthesized by anodic oxidation of copper through a simple electrolysis process employing plain water (with ionic conductivity, ~6 μS/m) as electrolyte. In this method no special electrolytes, chemicals and surfactants are needed. The method is based on anodization pursuant to the simple electrolysis of water at different voltages. Two different types of Cu_2O nanostructures have been found. One type got delaminated from copper anode and was collected from the bottom of the electrochemical cell and the other was located on the copper anode itself. The nanostructures collected from the bottom of the cell are either nanothreads embodying beads of different diameters, ~10–40 nm or nanowires (length, ~600–1000 nm and diameter, ~10–25 nm). Those present on the copper anode were nanoblocks with preponderance of nanocubes (nanocube edge, ~400 nm). The copper electrode served as a sacrificial anode for the synthesis of different nanostructures. Aligned ZnO nanorod array has been successfully synthesized by simple thermal evaporation catalyst free method. Detailed structural characterizations revealed that the as synthesized aligned ZnO nanorods are single crystalline, with a hexagonal phase, and with growth along the [0001] direction. The room-temperature photoluminescence spectra showed a weak ultraviolet emission at 380 nm, a broad blue band at 435 nm and a strong orange–red emission at 630 nm. Structural/microstructural characterization of these nanomaterials have been carried out employing scanning (XL-20) and transmission electron microscopic (Philips EM, CM-12 and Technai 20G^2) techniques and X-ray diffraction techniques having graphite monochromater with CuKα radiation (λ = 1·54439 Å) (X'Pert PRO PAN analytical). The UV-visible absorption spectra were recorded on Model–VARIAN, Cary 100, and Bio UV-visible spectrophotometer. The photoluminescence (PL) measurement was carried out at room temperature with a He–Cd, a laser excited at 325 nm.**

Keywords. **Nanostructured; Cu_2O nanostructures; electrolysis based oxidation; aligned ZnO nanorods.**

1. Synthesis of nanothreads, nanowires and nanocubes like structures of Cu_2O by electrolysis based oxidation of copper

1.1 *Introduction*

Copper oxide (Cu_2O) nanostructures have attracted significant attention as it is one of the first known *p*-type direct bandgap semiconductor (Briskman 1992) with a bandgap of 2·17 eV. This makes it a promising material for the conversion of solar energy into electrical or chemical energy (Grozdanov 1994). The growing interest in Cu_2O nanostructures is due to several reasons. Some of these are (i) Cu_2O is a potential photovoltaic material which is low cost, nontoxic and can be prepared in large quantities due to natural abundance of the base material, copper (Fernando *et al* 2001; Mathew *et al* 2001; Chen *et al* 2003), (ii) excitons created in Cu_2O have been shown as suitable candidates for Bose Einstein condensate because of the large exciton binding energy of 150 meV (Snoke 1996; Merizzi *et al* 2001; Johnson and Kavoulakis 2001) and (iii) Cu_2O has been reported to act as a stable catalyst for water splitting under visible light irradiation (Hara *et al* 1998; de Jongh *et al* 1999a, b). The Cu_2O nanostructures (Leopold *et al* 2002; Wang *et al* 2003; Gou and Morphy 2004; Chang *et al* 2005; Liu *et al* 2005) have been prepared by several methods such as electrodeposition (Barton *et al* 2001; Huang *et al* 2002), sonochemical method (Kumar *et al* 2001), thermal relaxation (Deki *et al* 1998), liquid phase reduction (Wang *et al* 2002) and vacuum evaporation (Yanagimoto *et al* 2001). Based on these approaches synthesis of Cu_2O nanostructures demands complex process control, high reaction temperatures, long reaction times, expensive chemicals and specific method for specific nanostructures.

1.2 *Experimental*

The process followed in the present investigation makes use of an inexpensive two-electrode (Pt: cathode, Cu:

*Author for correspondence (hepons@yahoo.com)

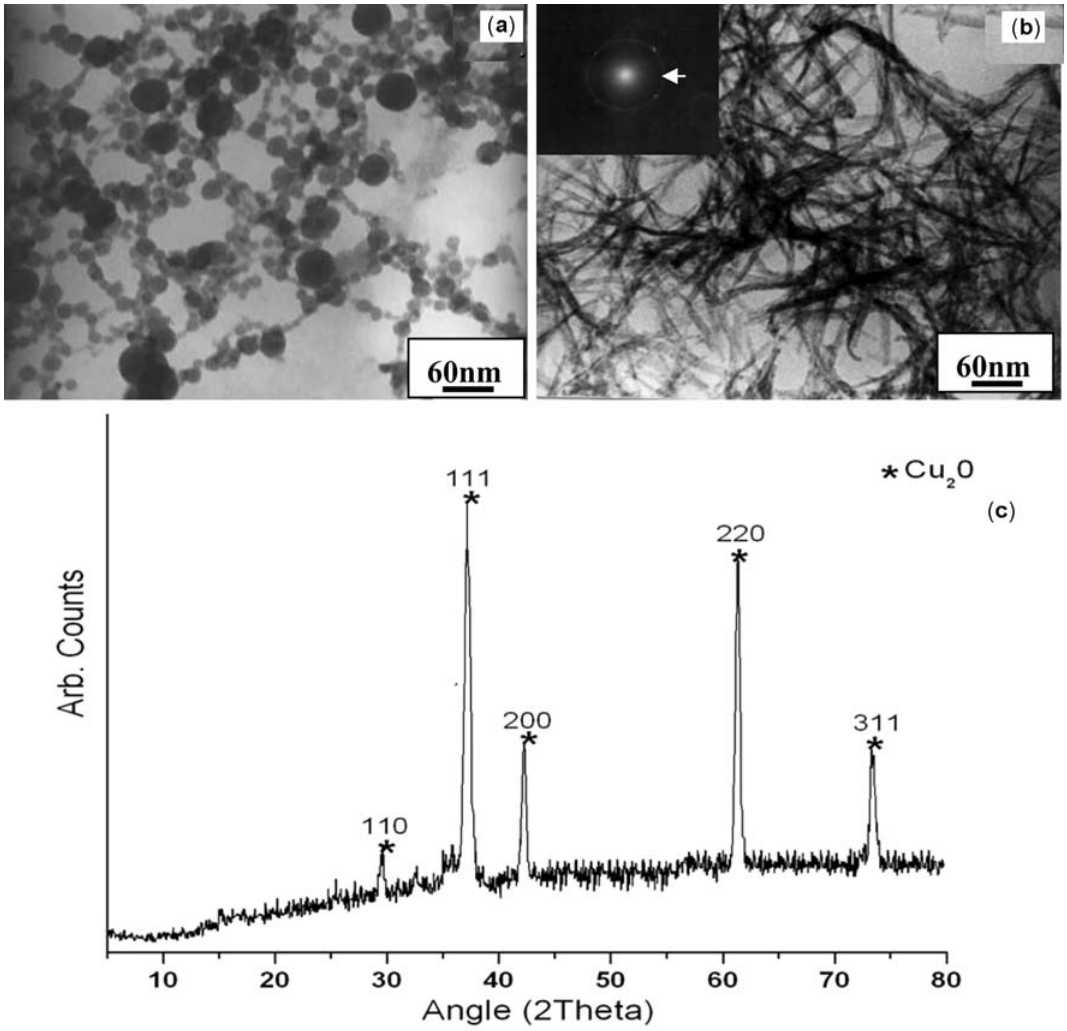

Figure 1. (**a**) Typical transmission electron micrograph of Cu_2O nanothreads embodying beads, as collected at the bottom of the cell after electrolysis at 2 V for 1 h, (**b**) is the representative TEM micrograph of dense Cu_2O network of nanowires, obtained after electrolysis at 6 and 10 V, respectively for 1 h and (**c**) is the X-ray diffraction of the as obtained materials at the bottom of the electrolytic cell after electrolysis at 6 V.

anode) setup with 5 ml of plain water as electrolyte. Copper works as a sacrificial anode and forms cuprous oxide nanostructures. Copper (99·9%) sheet (2 × 1 cm) as the anode and platinum sheet (2 × 1 cm) as cathode have been employed for the electrolysis. Before anodizing, the copper sheet was polished to a mirror finish with 0·2 μm alumina powder (in order to remove native oxide film) and then rinsed in distilled water. The distance between cathode and anode was kept at 1 cm. The electrolysis cell was made up of Perspex (4 × 3 × 3 cm) and the plain water (double distilled with very small ionic conductivity, ~6 μS/m and pH = 6·7) served as electrolyte. The electrolysis was performed at different applied voltages (2, 4, 6, 8 and 10 V) for 1 h.

1.3 *Results and discussion*

The morphology and microstructures of the particles obtained at different applied voltages have been investigated employing TEM. Figure 1(a) is a representative TEM micrograph of the particles obtained after electrolysis at 2 V for 1 h and collected from the bottom of the cell. Similar structures were obtained for 4 V. As can be seen, these represent nanothread-like structures of unspecified length comprising of nanobeads (bead size, ~10–40 nm). These structures revealed that the nanobeads coalesced together to form the nanothread. TEM image indicates that the nanothreads resulted due to the agglomeration of the bead-like particles.

Representative TEM micrograph of the material collected from the bottom of the cell after electrolysis at 6 V for 1 h is shown in figure 1(b). As can be seen, the Cu_2O structures here consist of nanowires (length, ~600–1000 nm and diameter, ~10–25 nm). It may be mentioned that the total length of Cu_2O nanothread and nanowire comprised of several segments. These were presumably formed due to interaction between nanothreads/nanowires forming the network in which the Cu_2O nanothread/nanowire configuration finally appears. When the electrolysis conditions were maintained at 10 V for 1 h, the representative TEM microstructure revealed the presence of dense Cu_2O nanowire network (length, ~1000 nm, diameter, ~10–25 nm). The X-ray diffraction pattern obtained from these nanomaterials, as shown in figure 1(c), could be indexed to a cubic system with lattice parameter, $a = 0{\cdot}4269 \pm 0{\cdot}005$ nm. These tally quite well with the lattice parameter of Cu_2O showing that the material formed under electrolysis conditions consist of cubic Cu_2O lattice structure.

In addition to the delaminated nanostructures, investigations of the copper anode, which were subjected to electrolysis runs, revealed the presence of another type of nanostructure of Cu_2O.

Figure 2(a) is the SEM image of the copper anode after electrolysis at 10 V for 1 h. At the lower voltages irregular block shaped structures were obtained which converted gradually into nearly cube shaped and perfect cube shaped particles at higher voltages. When the applied voltage was 10 V, regular cube-like microstructures were formed. Figure 2(a) exhibits typical nanocubes with cube edge, ~400 nm. This type of morphological changes in Cu_2O, bringing out block-like nanostructures have also been observed through *in situ* thermal oxidation in TEM (Zhou and Yang 2003). It may be pointed out that although the cube edge is rather large, keeping in view the nomenclature used by other workers (Gou *et al* 2003; Wang *et al* 2004), these may still be called nanocubes.

Figure 2(b) is the X-ray diffraction pattern of the treated copper sheet after the electrolysis run. The most intense peaks correspond to the (200) plane of copper substrate. Other peaks could be indexed to a cubic system with lattice parameter, $a = 0{\cdot}4269 \pm 0{\cdot}005$ nm. These tallies quite well with the lattice parameter of Cu_2O showing that the nanocubes like material formed at the copper sheet after electrolysis corresponds to cubic Cu_2O lattice structure. The electrochemical situation in the present case (Pt/water (mildly acidic)/Cu) with applied voltage always larger than ~1·23 V correspond to electrolysis with moderate to vigorous oxygen (and hydrogen) evolution.

Under the electrolysis condition a continuous layer of adsorbed oxygen on Cu anode is expected. This would be termed as adsorbed oxygen $[O]_{ads}$ (where SA stands for surface adsorbed species). They can combine to form O_2, which evolves as oxygen. The anode (Cu) will generate Cu^{2+} which on reacting with the $(O–O)_{SA}$ will form Cu_2O.

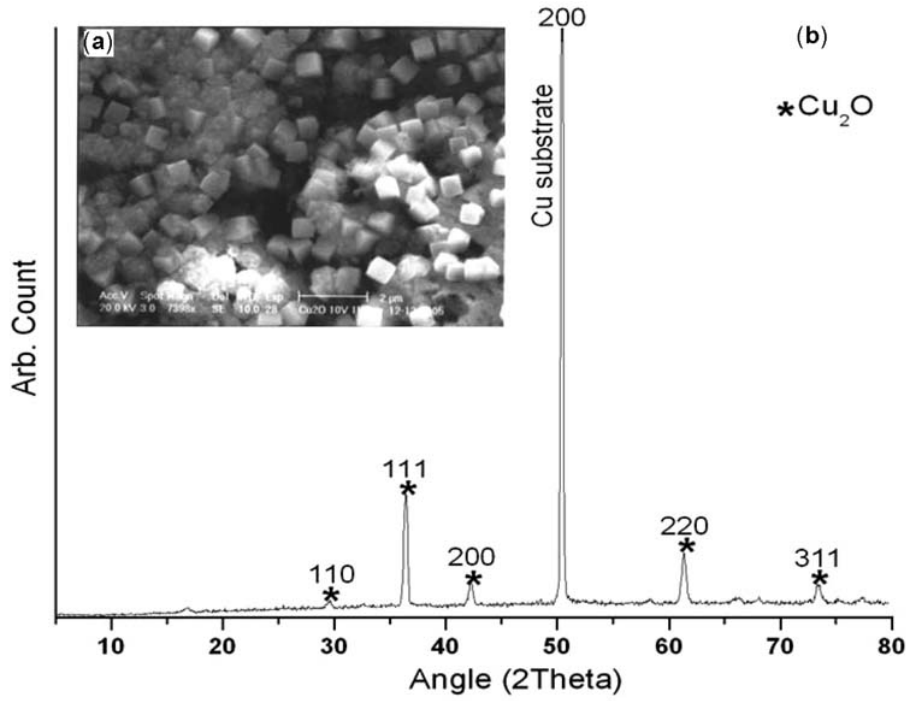

Figure 2. (**a**) SEM micrographs of the copper electrode after electrolysis at 10 V and (**b**) XRD pattern of the copper sheet after electrolysis at 10 V for 1 h.

As regards the formation of nanocubes on the surface of the copper anode, we propose that these are formed when copious oxygen produced through electrolysis attacks comparatively large regions/blocks of copper anode (~400 nm). These regions may be pits or surface inhomogeneities etc. Here, similar to the formation of nanowires as described earlier, Cu_2O block nanostructures, an overgrowth on copper anode will result. We propose that the higher applied voltage (e.g. 8 V or 10 V) for electrolysis represents the optimum conditions for the formation of nanocubes. These nanocubes reflect the basic cubic unit cell of Cu_2O.

We recorded the UV-visible absorption spectra of the nanothreads and nanowires like structures synthesized in electrolyte medium at 2 and 6 V. The samples were well dispersed in distilled water to form a homogeneous suspension. Figures 3a–c show the absorption spectra and corresponding bandgap calculations of the as synthesized samples at 2 and 6 V, which show broad absorption peaks at 365 nm and 361 nm, respectively. An estimate of the optical bandgap is obtained using the following equation for a semiconductor (Subramanian *et al* 2002)

$$A = \frac{K(h\nu - E_g)^{m/2}}{h\nu}, \quad (1)$$

where A is the absorbance, K a constant and m is equal to 1 for direct transition and 2 for indirect transition. Figures 3(b) and (c) show a plot of $(Ah\nu)^2$ vs E_{phot} (for nanothreads and nanowires) for a direct transition, and the value of E_{phot} extrapolated to $A = 0$ gives an absorption edge energy which corresponds to bandgap, E_g.

The bandgap of as prepared Cu_2O nanothreads and nanowires is estimated to be 2·61 and 2·69 eV from the UV-visible absorption spectrum, which is larger than the direct bandgap (2·17 eV) of bulk Cu_2O (Wang and Searson 1999). The higher bandgap can be attributed to size effect of the present nanostructures. Thus the increase of bandgap as compared to the bulk can be understood on the basis of quantum size effect which arises due to very small size of nanothreads and nanowires in one-dimension.

2. Synthesis of aligned nanorods of ZnO by thermal evaporation method

2.1 *Introduction*

Application of semiconductor nanostructures in devices is one of the major aims of recent nanoscience researchers. This requires the preparation of nanostructures with controlled crystalline morphology, orientation and surface architecture. Extended and oriented nanostructures are desirable for many applications, including microelectronics devices, chemical and biological sensing and diagnosis, energy conversion and storage (photovoltaic cells, batteries, capacitors devices and hydrogen storage), light emitting displays, catalysis, drug delivery and optical storage (Wang 2004; Jagdish and Pearton 2006). Previously, oriented carbon nanotubes (Srivastava *et al* 2004) and oriented oxide nanorods were prepared by high temperature vacuum deposition techniques. Similar techniques were used for making nanowires of Si and silicon carbine/nitride and nanobelts of a wide range of oxide materials.

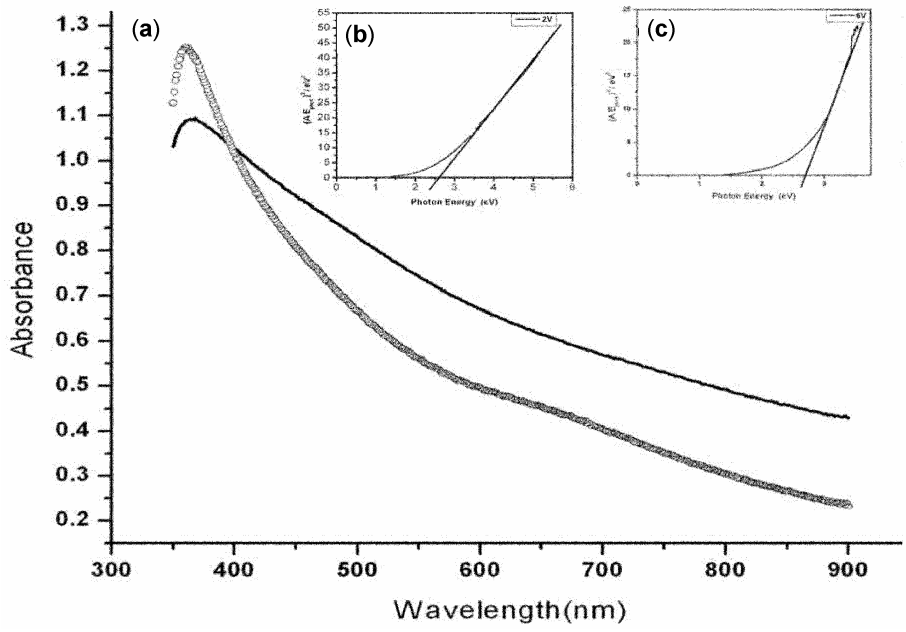

Figure 3. (**a**) UV-visible absorption spectrum of the nanothreads and nanowires like structures synthesized at 2 V and 6 V, (**b**) and (**c**) bandgap calculation of the nanothreads and nanowires like structures from the UV-visible absorption spectrum.

Recently, synthesis through physical vapour deposition employing catalysts and electrochemical deposition in porous membranes were also investigated to produce aligned ZnO nanorods and tubes (Wang 2004; Jagdish and Pearton 2006). Although aligned nanowire and nanorods have attracted wide attention, direct fabrication of large arrays of complex nanostructures with controlled crystalline morphology and orientation remains a significant challenge.

ZnO is an important semiconducting material with many useful properties such as piezoelectricity, conductivity, optical absorption and emission, high voltage–current nonlinearity, sensitivity to gases and chemical agents and catalytic activity (Wang 2004; Ozgur *et al* 2005; Chakravorty *et al* 2006). It has been extensively investigated for applications in luminescence and as window and electrode material for solar cells, piezoelectric actuators, micro/nanosensors, photocatalysts, hydrogen storage (Ozgur *et al* 2005) and so on. The properties of ZnO depend closely on the microstructures of the materials, including crystal size, orientation and morphology, aspect ratio and even crystalline density. The surface area and morphology also have a crucial role in many applications such as photoemitters, sensors, catalysts and field emitters. In field emission, for example, an array of densely packed nanorods greatly reduces the field enhancement effect at the tip of the rod to a level not much different from a flat, while too loosely distributed nanorods cannot meet the desired requirement of high emitting points.

ZnO is a wide bandgap (~3·3 eV at room temperature) with large (~60 meV) exciton binding energy semiconductor, which is of interest for a great variety of practical applications, including short-wavelength photonic devices. Therefore, the optical properties of ZnO have been extensively studied (Wang 2004; Ozgur *et al* 2005). In addition to UV excitonic emission peak, ZnO commonly exhibits visible luminescence at different emission wavelengths due to intrinsic or extrinsic defects. The most commonly observed green emission is the most controversial one, for which various hypotheses have been proposed. On the other hand, orange–red emission has been less commonly observed than green and yellow emissions.

In this paper, we report the controlled growth of aligned ZnO nanorods using simple thermal evaporation of Zn in oxygen ambience without any catalyst and with argon as the carrier gas. In order to identify the growth conditions from aligned nanorods, we have performed a study of the effects of the various parameters that affect the growth and morphology. Specifically, we have investigated the effects of mass of Zn flux: temperature on the growth zone in the furnace, flow rate of carrier gas and oxygen gas. Therefore, we have adopted these conditions for the growth of aligned nanorods reported in this paper.

2.2 *Experimental*

Simple thermal evaporation technique was used to grow aligned ZnO nanorods without any catalysts and vacuum system. High purity Zn metal powders were used as the starting material. The growth process was performed inside a horizontal tube furnace. Pure Zn metal powder (99·99%, 325 mesh) was heated at a temperature of 900°C for ~10–15 min in a mixed environment of argon (carrier gas) and oxygen (reactive gas) flowing at 500 and 300 standard cubic centimeters per min (SCCM), respectively on an alumina boat. The ZnO nanostructures were found to grow on the alumina boat. Scanning electron microscopic investigations reveal these nanostructures to be aligned ZnO nanorods.

2.3 *Results and discussion*

In our previous work, controlled self-assembled growth of ZnO nanotetrapods: nanorods, nanoflowers and nanoparti-

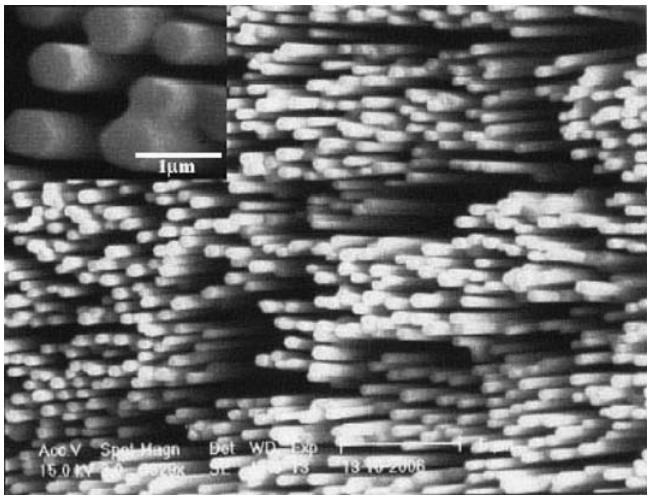

Figure 4. A low magnification SEM image of the aligned ZnO nanorods. The inset is the high magnification SEM image.

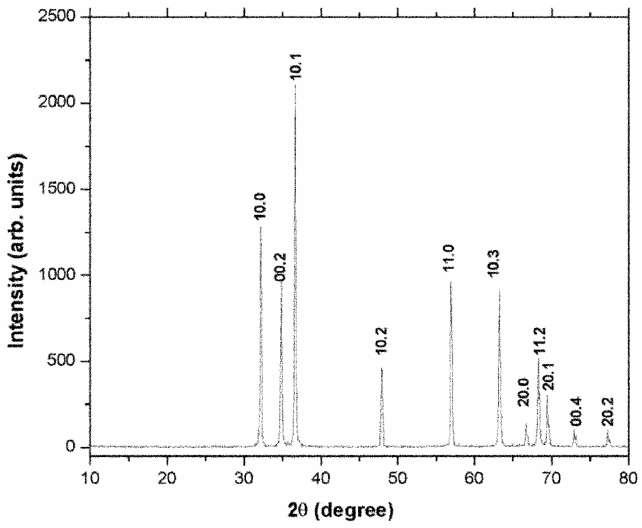

Figure 5. XRD pattern of as-grown ZnO sample.

cles, were synthesized by simple oxidation of Zn powder (Singh *et al* 2005, 2007). By varying experimental conditions, large embodying aligned ZnO rods could be obtained. A representative SEM image of the ZnO nanorods fabricated on alumina boat at 900°C is shown in figure 4. As shown in the image, the ZnO nanorods are well aligned and uniform on a large scale. The inset in figure 4 is a high magnification SEM image, which shows that the nanorods have hexagonal tip with a diameter of about 450 nm.

The gross structural characteristics of the aligned ZnO nanorods was carried out through XRD (a representative XRD pattern is given in figure 5). This confirmed that the as grown material is ZnO with hexagonal wurtzite structure (JCPDS 36-1451). In addition, no diffraction peaks from Zn could be found revealing that ZnO phase was the singular phase formed.

The possible growth mechanism of the aligned nanorod arrays is vapour–solid (VS) mechanism, because no metal catalysts are used in the whole evaporation procedure. So the growth is different from the traditional vapour–liquid–solid (VLS) mechanism. But the mechanism of aligned growth of ZnO is still an open question and needs more study. Many mechanisms have been developed such as constraint of the pores in either mesoporous silicon or porous anodic alumina, van der Waals interaction, effects of d.c. bias and so on. In this work, we have synthesized well-aligned ZnO nanorods apparently nucleated via a self-catalysed growth mechanism. Here, we propose a growth mechanism for the aligned ZnO nanorods, where the growth could be separated into two stages. The first stage is the growth of ZnO nuclei as stoichiometric and later it transforms to ZnO_x, through creation of oxygen vacancies (Srivastava *et al* 2005). The second stage is the growth of ZnO_x which acts as self-catalyst and leads to the formation of aligned ZnO nanorods along [0001] direction. By scanning tunneling microscopy, it has been shown that the clean (0001)-Zn faces roughen across two atomic layers in order to stabilize themselves by non-stoichiometry (Dulub *et al* 2003).

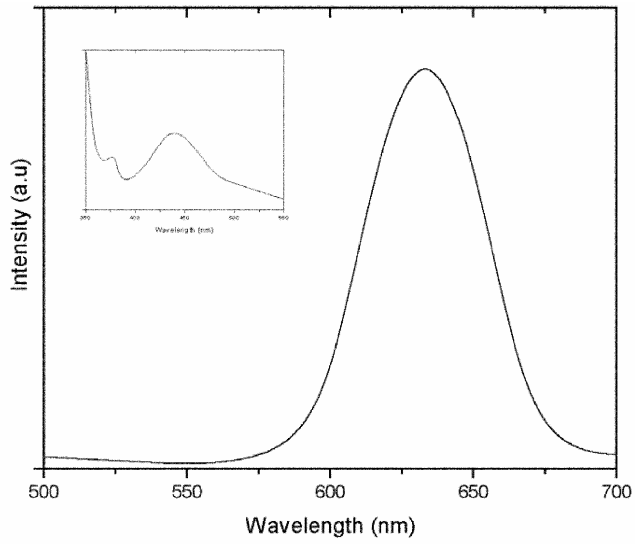

Figure 6. Room temperature photoluminescence (PL) spectra of the aligned ZnO nanorods.

The photoluminescence of the as grown well aligned ZnO nanorod was examined with a He–Cd laser of 325 nm at room temperature. Figure 6 shows a typical PL spectrum, which exhibits a weak UV emission at 380 nm, a broad blue emission at 435 nm, and a strong orange–red emission at 630 nm. The ultraviolet band is attributed to the band-edge exciton recombination and the visible band is related to the defects in ZnO nanostructures. Considering the intrinsic point defect state levels in the energy band of ZnO, the peak at 630 nm is probably caused due to (i) transition from the monovalent interstitial zinc (Zn_i^+) or oxygen vacancy (V_O^+) to the monovalent vacancies (V_O^+) and (ii) transition from the conduction band to the monovalent vacancies (V_O^+). The UV emission originated from the excitonic recombination corresponding to the band edge emission of ZnO. The origin of blue emission from the undoped ZnO is associated with the intrinsic defect centres such as oxygen vacancy (V_O), zinc vacancy, or oxygen interstitial. Obviously, by controlling the morphology of ZnO nanostructures, the optical property of ZnO nanostructures can be tunable, which will be useful for nanolaser applications.

3. Conclusions

Based on the results of present investigations, the following conclusions can be drawn:

(I) We are able to synthesize different possible nanostructures (nanothreads, nanowires and nanocubes) of Cu_2O by a very simple and inexpensive method of water electrolysis induced by anodization of copper electrode. The present method, in contrast to other known processes, of the formation of Cu_2O nanostructures does not require special electrolytes, chemicals or surfactants. The calculated optical bandgap of the as prepared Cu_2O nanostructures (nanothread and nanowires) at 2 V and 6 V from the UV-visible absorption spectra corresponds to 2·61 and 2·69 eV, which are larger than the direct bandgap (2·17 eV) of bulk Cu_2O.

(II) Aligned ZnO nanorods have been synthesized by oxygen assisted thermal evaporation of metallic zinc on an alumina boat. A self-catalyzed process is believed to be operative here. The room-temperature photoluminescence spectra showed a weak ultraviolet emission at 380 nm, a broad blue band at 435 nm, and a strong orange–red emission at 630 nm.

Acknowledgements

The authors are extremely grateful to Prof. A R Verma, Prof. C N R Rao (FRS, Chairman, Nanoscience and Tech-

nology Mission, Govt. of India), Prof. A K Raychaudhary, Prof. A K Sood and Prof. P M Ajayan (RPI, USA) for their encouragement, support and fruitful discussions. The authors acknowledge with gratitude the financial support from the DST (UNANST: BHU), CSIR, UGC and MNRE.

References

Barton J K, Vertegal A A, Bohannan E W and Switzer J A 2001 *Chem. Mater.* **13** 952

Briskman R N 1992 *Sol. Energy Mater. Sol. Cells* **27** 361

Chang Y, Teo J J and Zeng H C 2005 *Langmuir* **21** 1074

Chen Z Z, Shi E W, Zheng Y, Li W J, Xiao B and Zhuang J Y 2003 *J. Cryst. Growth* **249** 294

de Jongh P E, Vanmaekelbergh D and Kelly J 1999a *J. Chem. Commun.* 1069

de Jongh P E, Vanmaekelbergh D and Kelly J 1999b *J. Chem. Mater.* **11** 351

Deki S, Akamatsu K, Yano T, Mizuhata M and Kajinami A 1998 *J. Mater. Chem.* **8** 1865

Dulub O, Diebold U and Kresse G 2003 *Phys. Rev. Lett.* **90** 016102

Fernando C A N, De Silva L A A, Mehra R M and Takahashi K 2001 *Semicond. Sci. Technol.* **26** 433

Gou L and Morphy C J 2004 *J. Mater. Chem.* **14** 735

Grozdanov I 1994 *Mater. Lett.* **19** 281

Hara M, Kondo T, Komodo M, Ikeda S, Shinohara K, Tanaka A, Kondo J N and Domen K 1998 *Chem. Commun.* 357

Huang L N, Wang H T, Wang Z B, Mitra A, Zhao D Y and Yan Y S 2002 *Chem. Mater.* **14** 876

Jagdish C and Pearton S 2006 *Zinc oxide bulk, thin films and nano structures processing, properties and applications* (Oxford: Elsevier)

Johnson K and Kavoulakis G M 2001 *Phys. Rev. Lett.* **86** 858

Kar S, Pal B N, Chaudhari S and Chakravorty D 2006 *J. Phys. Chem.* **B110** 4605

Kumar R V, Mastai Y, Diamant Y and Gedanken A 2001 *J. Mater. Chem.* **11** 1209

Leopold S, Schuchert I U, Lu J, Molares M E T, Merranen M and Carlsson J O 2002 *Electrochim. Acta* **47** 4393

Liu Y L, Liu Y C, Mu R, Yang H, Shao C L, Zhang J Y, Lu Y M, Shen D Z and Fan X W 2005 *Semicond. Sci. Technol.* **20** 44

Mathew X, Mathew N R and Sebastian D J 2001 *Sol. Energy Mater. Sol. Cells* **70** 277

Merizzi A, Masse M and Fortin E 2001 *Solid State Commun.* **120** 419

Ozgur U, Alivov Y I, Liu C, Teke A, Reshchikov M A, Dogan S, Aurutin V, Cho S J and Morkoc H 2005 *Appl. Phys. Rev.* **98** 043101

Singh J, Srivastava A, Tiwari R S and Srivastava O N 2005 *J. Nanosci. Nanotechnol.* **5** 2093

Singh J, Tiwari R S and Srivastava O N 2007 *J. Nanosci. Nanotechnol.* **7** 1783

Snoke D 1996 *Science* **273** 1351

Srivastava A, Srivastava O N, Talapatra S, Vajtai R and Ajayan P M 2004 *Nat. Mater.* **3** 610

Subramanian B, Sanjeeviraja C and Jayachandran M 2002 *J. Cryst. Growth* **234** 421

Wang E M and Searson P C 1999 *Appl. Phys. Lett.* **74** 2939

Wang W, Wang G, Wang X, Zhan Y, Liu Y and Zhang C 2002 *Adv. Mater.* **14** 67

Wang W, Varghese O K, Ruan C, Paulose M and Grimes C A 2003 *J. Mater. Res.* **18** 2754

Wang Z, Chem X, Liu J, Mo M, Yang L and Qian Y 2004 *Solid State Commun.* **130** 585

Wang Z L 2004 *J. Phys. Condens. Matter* **16** R829

Yanagimoto H, Akamatsu K, Gotoh K and Deki S 2001 *J. Mater. Chem.* **11** 2387

Zhou G and Yang J C 2003 *Appl. Surf. Sci.* **210** 165